International Journal of Non-Linear Mechanics 118 (2020) 103280

Contents lists available at ScienceDirect

International Journal of Non-Linear Mechanics

journal homepage: www.elsevier.com/locate/nlm

A parametric study on the nonlinear dynamic response of paper-based mechanical systems due to liquid transport

Isaias Cueva-Perez [a], Angel Perez-Cruz [a], Ion Stiharu [b], Aurelio Dominguez-Gonzalez [a], Miguel Trejo-Hernandez [a], Roque Alfredo Osornio-Rios [a,*]

[a] Mecatrónica/Facultad de Ingeniería, Campus San Juan del Rio, Universidad Autónoma de Querétaro, Rio Moctezuma 249, Col. San Cayetano, 76807 San Juan del Rio, Querétaro, Mexico

[b] Department of Mechanical and Industrial Engineering, Concordia University, 1455 De Maisonneuve Blvd. W. Montreal, Quebec, Canada H3G 1M8

ARTICLE INFO

Keywords:
Paper-based structures
Cantilever beam
Water transport
Dynamic response
Parametric study
Bending response
Relaxation

ABSTRACT

In recent years, the mechanical response of paper when interacting with liquids has been investigated. Nonlinear phenomena inherent to paper-liquid interaction such as the Young modulus relaxation, hygrostrain and liquid transport have been considered. However, the mechanical response of paper has only been studied for a static or quasi-static bending response. In this work, a parametric study is presented to study the dynamic response of paper-based mechanical systems interacting with liquids. A three-dimensional multiphysics model is implemented and solved in COMSOL® to couple the liquid transport and the mechanical response problem. The Richard's model and an elasticity formulation are used to describe the liquid transport and the mechanical problem respectively. Three parameters are selected from this model in order to describe the dynamic response of paper. The influence of each parameter on the dynamic response is also determined. This model is validated experimentally with resonance frequency measurements on paper-based cantilever beams using three water–ethanol solutions. The results show that this model can be used to describe the drying process of paper-based devices under dynamic loads. This study can lead to the development of low-cost devices for liquid characterization.

1. Introduction

In recent years, paper-based devices have emerged as an interesting alternative in the development of sensors and actuators due to its properties, such as low weight, low fabrication cost, disposability, high-availability and capillarity. The development of these devices started with the introduction of electro-active polymer actuators in 2000 [1]. In this work, Kim et al. developed an actuator consisting of a paper element sandwiched between two electrodes. Since then, different attempts to develop paper mechanical devices have been done. For instance, Ding et al. [2] fabricated paper-based magnetic actuators with paper as a structural material and a ferromagnetic fluid to produce actuation. In another work, Fraiwan et al. [3] implemented a naked-eye detection sensor for gas detection consisting of an array of paper-based cantilever beams fixed within a frame. Paper-based mechanical devices have been also developed for static force sensing. Meanwhile, Liu et al. [4] built an inertial sensor with chromatography paper as a substrate and printed carbon resistors as sensing element. In another example, Ren et al. [5] developed a force sensor using office paper with a printed graphite piezoresistor over the paper substrate. In a recent development, Wang et al. [6] constructed a paper-based piezoelectric accelerometer. This device is made with a card stock paper substrate and ZnO-NWs (zinc oxide nanowires) coated paper. These works paid little attention to mechanical properties of the paper substrates such as bending stiffness or elastic modulus.

In this respect, different studies focusing on the mechanical properties of paper can be found in the open literature. For example, Erkkilä et al. [7] proposed two models that correlate the elasto-plastic behavior and hygroexpansion-shrinkage of paper with few manufacturing parameters. Gao et al. [8] studied the creep and relaxation phenomena of Chinese calligraphy paper under stretching loads. The authors used Burgers model to describe creep behavior and a five-element Maxwell model to describe the relaxation. In another example, Li et al. [9] developed an elasto-plastic model to describe the nonlinear behavior of laminated paper. A set of experiments with paper samples was performed to calibrate the elasto-plastic parameter models. Hall et al. [10] studied the elastic behavior of aged paper by performing nondestructive deflection tests on paper strips held horizontally. Properties such as the bending and the elastic moduli were obtained by fitting the deflection profiles of the strips to nonlinear bending theories. These works provided a better understanding of the mechanical response of paper under static or quasi-static loads.

* Corresponding author.
E-mail address: raosornio@hspdigital.org (R.A. Osornio-Rios).

https://doi.org/10.1016/j.ijnonlinmec.2019.103280
Received 4 June 2019; Received in revised form 29 August 2019; Accepted 18 September 2019
Available online 27 September 2019

Nomenclature

b	Beam width [m]
$D(\varphi)$	Moisture diffusivity [m^2s^{-1}]
D_0	Equivalent diffusivity constant [m^2s^{-1}]
$E(x, y, z, \varphi)$	Young modulus as a function of moisture content [N m^{-2}]
E_{dry}	Young modulus of dry paper [N m^{-2}]
e_a	Absolute error
e_{RMS}	Root mean square error
f	Sink/Source term [1/s]
F	Normalized sink/source term
f_r	Resonance frequency [Hz]
f_{ss}	Dry resonance frequency [Hz]
f_n	Normalized resonance frequency
h	Beam thickness [m]
J	Elasticity tensor
l	Beam length [m]
m	Ratio between saturated and dry Young modulus
n	Power of diffusivity function
P_t	Dimensionless paper porosity
r_{ex}	Normalized experimental resonance frequency
S	Stress tensor [N m^{-2}]
T	Dimensionless time
T_s	Steady state constant
u	Displacement vector [m]
V_a	Sample apparent volume [m^3]
V_{sol}	Saturation liquid volume [m^3]
x, y, z	Space coordinates [m]
X, Y, Z	Material coordinates [m]

Greek symbols

β	Relaxation constant
ε	Total strain tensor
ρ	Paper density [kg m^{-3}]
τ	Time constant [s]
ϕ	Dimensionless moisture content
φ(x,y,z,t)	Moisture content [m^3m^{-3}]
φ_s	Saturated moisture content [m^3m^{-3}]
ω	Eigen frequency [rad/s]

The internal structure of paper provides an excellent medium to transport liquids without an external force. Furthermore, the absorbency of paper enables the possibility of the storage of reagents inside paper. Paper-based microfluidic devices make use of these properties, enabling its usage in applications such as substance detection, bioassays, colorimetric analysis, medical diagnosis, environmental testing and food quality testing [11]. Some authors have studied the changes in the mechanical properties of paper caused by the interaction with liquids. For instance, Douezan et al. [12] proposed a parameter model to study the curling of wet tracing paper. The authors also determined the Young modulus for saturated paper and dry paper. In another work, Reyssat et al. [13] studied the mechanical response of tracing paper due to water interaction phenomena such as swelling and liquid transport. The authors related the curvature of the paper sample with the changes in thickness and Young modulus of the paper. The Young modulus is described with an empirical form that fits an exponential function in terms of the water content. In another example, Lee et al. [14] quantified the geometry and mechanics of filter paper when it imbibes water from a capillary. The Young modulus was co-related to its wetness by measuring the tensile stress and strain using a tensile meter. Perez et al. [15] proposed a two-dimensional imbibition model of paper-based networks using the nonlinear Richard's equation for unsaturated porous media. The numerical solution of this model provided the unsaturated distribution of liquid inside paper. In another example, Perez et al. [16] studied the bending response of paper beams due to water imbibition. The authors proposed a model that considers three hygro-mechanical phenomena: water imbibition, fiber swelling and the softening effect in paper due to water interaction. The bending response of paper was characterized using only four parameters. It should be noticed that this works only provide a description of the interaction of paper with liquid from a static or quasi-static approach. However, the increasing applications of paper-based mechanical systems demands more knowledge about the dynamic behavior of the wet paper. Furthermore, it is known from the literature that the mechanical behavior of wet paper can be considered as a combination of nonlinearities such as the relaxation of the material and the liquid transport [16].

In this work, a parametric study of the dynamic response of paper-based mechanical systems due to its interaction with liquids is presented. A three-dimensional multiphysics model is implemented and solved numerically in COMSOL® to couple the physics of the liquid transport problem and the mechanical problem. The liquid transport is described with the nonlinear Richard's model for porous media to determine the liquid concentration in a paper-based cantilever beam. The dynamic response of the beams is described using three parameters from the multiphysics model: (i) the relaxation constant of the material β, (ii) the ratio between the saturated and dry Young modulus m and (iii) the normalized sink/source term F. A numerical analysis is carried out in order to determine the individual influence of these parameters in the dynamic response of the beam. The model is experimentally validated with three aqueous solutions of with 0%, 25% and 50% volume of ethanol. The results show that the drying process in paper subjected to dynamic loads can be accurately characterized despite the nonlinearities and complexity of the physical phenomena involved. This study can lead to the development of low-cost devices for the characterization of different liquids.

2. Modeling

Let us consider a generic paper-based cantilever beam as shown in Fig. 1 with length l, width b and thickness h initially saturated with a water-based liquid. Some phenomena must be considered to study the dynamic response of the beam during a drying process. First, the liquid interacts with the paper fibers, thus producing a relaxation of the Young modulus as the water acts as a plasticizer [17]. Second, a moisture gradient is produced as the top ($z = h$) and bottom ($z = 0$) surfaces of the beam which are exposed to an ideal zero-moisture concentration. The transport phenomena through the lateral surfaces of the beam is neglected as the area of lateral surfaces is negligible in comparison with the top and bottom surfaces.

A three-dimensional liquid transport–solid mechanics model is used to analyze the response of a paper-based cantilever beam under dynamic loads with the following assumptions. (i) The liquid is transported to the top and bottom surfaces of the beam, (ii) The liquid transport is a nonlinear three-dimensional transport problem from a saturated state to a completely dry state. (iii) The effects of expansion/shrinking of the fibers, hydrostatic pressure and inertial forces are neglected. (iv) Paper is a linear elastic material. (v) The Young modulus of paper depends on the moisture concentration.

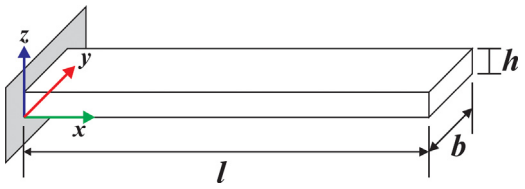

Fig. 1. Geometry of the paper-based cantilever beam.

2.1. Liquid transport

The changes in the mechanical properties of paper related to liquid transport could be captured by using a suitable, three-dimensional transport model. The nonlinear Richard's model is used in this study as it has been used in the literature to describe liquid flow in porous media. The suitability of this model in describing liquid transport in paper has already been discussed in [15]. For a three-dimensional unsaturated porous media, the Richard's model that formulates the liquid concentration is presented in Eq. (1)

$$\frac{\partial \varphi}{\partial t} - \frac{\partial}{\partial x}\left(D(\varphi)\nabla\varphi\right) - \frac{\partial}{\partial y}\left(D(\varphi)\nabla\varphi\right) - \frac{\partial}{\partial z}\left(D(\varphi)\nabla\varphi\right) = f \tag{1}$$

where $D(\varphi)$ is the moisture diffusivity, $\phi(x, y, z, t)$ is the moisture content in the position (x, y, z) at an instant t (see Fig. 1) and f is the sink/source term that represents the liquid inflow or outflow. The initial condition is $\varphi(x, y, z, 0) = \varphi_s$, where φ_s is the moisture content at saturation; the boundary conditions are zero liquid content ($\varphi = 0$) in $z = 0$ and $z = h$, and a nonflux condition at the lateral surfaces where $x = 0, x = l, y = 0$ and $y = b$. It must be considered that a discontinuity is present in the interfaces at $z = 0$ and $z = h$ as the value of φ suddenly rises to φ_s at $t = 0$; thus incrementing the complexity of the model. $D(\varphi)$ represents the moisture diffusivity and can be described in a Richard's equation framework by the Eq. (2) [16].

$$D(\varphi) = D_0\varphi^n \tag{2}$$

where D_0 represents and equivalent diffusivity constant, and the order n is related to the pore size distribution of paper [16]. In this study, a value of $n = 6$ is used, according to the results obtained in [16] when modeling the liquid transport process in paper with Richard's model.

2.2. Elasticity model

In this study, the paper-based cantilever beam is modeled as a linear elastic element. The stress and deformation state are referred to the total Lagrangian formulation. In this formulation, when a body is deformed, the material coordinates of the body $\boldsymbol{X}$ remain unchanged. The spatial coordinates $\boldsymbol{x}$ change with the applied forces and time as presented in Eq. (3)

$$\boldsymbol{x} = \boldsymbol{X} + \boldsymbol{u}(\boldsymbol{X}, t) \tag{3}$$

where $\boldsymbol{u}$ represents the displacement vector. The global cartesian components in the directions of x, y and z are defined as u, v, and w respectively. Hence the displacement gradient is defined as:

$$\nabla\boldsymbol{u} = \begin{bmatrix} \frac{\partial u}{\partial X} & \frac{\partial u}{\partial Y} & \frac{\partial u}{\partial Z} \\ \frac{\partial v}{\partial X} & \frac{\partial v}{\partial Y} & \frac{\partial v}{\partial Z} \\ \frac{\partial w}{\partial X} & \frac{\partial w}{\partial Y} & \frac{\partial w}{\partial Z} \end{bmatrix}$$

In this elasticity formulation, it is assumed that the beam undergoes small deflection in pure bending. Therefore, the total strain tensor is written in terms of the displacements as shown in Eq. (4)

$$\varepsilon = \frac{1}{2}\left(\nabla\boldsymbol{u} + \nabla\boldsymbol{u}^T\right) \tag{4}$$

Hence, the stress tensor $\boldsymbol{S}$ for a linear elastic material can be expressed as follows:

$$\boldsymbol{S} = J : \varepsilon \tag{5}$$

where J is the fourth order elasticity tensor and ':' represents the double dot tensor product. In the context of this formulation, the dynamic behavior of the beam can be described by Eq. (6) as follows:

$$-\rho\omega^2\boldsymbol{u} = \frac{\partial \mathbf{S}}{\partial x} + \frac{\partial \mathbf{S}}{\partial y} + \frac{\partial \mathbf{S}}{\partial z} \tag{6}$$

where ρ represents the density of the material and ω represents the eigenfrequencies of the beam.

For this study, the Young modulus is dependent on the liquid concentration. For this study, an empirical function based on the experimental results observed in [14] is proposed. This function is represented in Eq. (7)

$$E(x, y, z, \varphi) = \frac{E_{dry}}{m^{-1} + \left(1 - m^{-1}\right)e^{-\beta\varphi(x,y,z,t)}} \tag{7}$$

where E_{dry} is the Young modulus of dry paper, m is the ratio between the saturation Young modulus and $E_{dry,}$ and β is a relaxation constant that determines the dynamic of the transition between wet and dry states. From an analysis of this equation, it can be observed that the Young modulus has a nonlinear behavior due to its dependence on the liquid-transport solution.

2.3. Model parameters

Four parameters are initially considered to describe the dynamic response of a paper-based cantilever beam as follows. (i) Two parameters that govern the liquid transport; the equivalent diffusivity constant D_0 and the sink/source term f, and (ii) two parameters that define the behavior of the Young modulus; the relaxation constant β and the ratio between wet and dry Young modulus m. A difference with the formulation presented in [16] can be noticed, as the sink/source term was not considered to describe the liquid transport.

In order to simplify the analysis in this study, the following sets of normalized parameters are introduced

$$\phi = \frac{\varphi}{\varphi_s} \tag{8a}$$

$$T = \frac{t}{\tau} \tag{8b}$$

where τ represents the time constant of the problem. Using a similar approach as in [16], the time-scale can be represented by the following expression as

$$\tau = \frac{h^2}{D_0\varphi_s} \tag{9}$$

In this manner, the parameter D_0 can be discarded as it is now implicitly included in the parameter τ. The sink/source parameter f can be rewritten to be described in terms of the time constant τ as follows:

$$F = f\tau \tag{10}$$

Thus, the initial condition for the concentration is represented as

$$\phi(x, y, z, 0) = 1 \tag{11a}$$

and the boundary conditions are represented as

$$\phi(x, y, 0, T) = 0 \tag{11b}$$

$$\phi(x, y, h, T) = 0 \tag{11c}$$

3. Materials and methods

The numerical approach used to obtain the dynamic response of the multiphysics model is described in this section. A parametric analysis is performed to determine the individual influence of the three parameters on the dynamic response of the model. An experimental validation is also presented to check the validity of this parametric study.

Table 1
Values for the parametric study.

Parameter	Values used
$F(1/s)$	-1×10^{-3}, -1×10^{-1}, -10
β	1, 8
m	1×10^{-3}, 1×10^{-2}, 1×10^{-1}, 1

3.1. Numerical solution

The multiphysics model (liquid transport and elasticity) is implemented and solved by COMSOL to determine the dynamic response of the beam. A numerical model is used considering the complexity of the phenomena involved in this study, such as the dependence of the mechanical properties on the spatial distribution and time variation of the concentration. A Coefficient Form PDE (Partial Differential Equation) model is implemented to describe the liquid transport phenomena based on Eq. (1) using the normalized sink/source parameter F. A Solid Mechanics model is implemented to describe the mechanical behavior of the cantilever beam using the ratio of the wet and dry Young modulus m and the relaxation constant β. Eq. (7) is implemented in this model to describe the Young modulus of paper with the concentration ϕ. It is important to point out that hygroscopic strain is not considered in this model as microscopic scale effects are not studied. It is expected that this model can be used to determine the dynamic response of the beam using only the parameters F, m and β. A fixed boundary condition is added in one end of the beam where $x = 0$. Furthermore, a mass per unit of volume dependent on the concentration ϕ is also added to the beam domain to represent the liquid mass on the beam.

The solution of the problem is obtained in 2 steps. First, a time-dependent study is used to determine the concentration $\phi(x, y, z)$ at an instant t. Secondly, an eigenfrequency study for the first flexural vibration mode is performed to obtain the resonance frequency f_r at an instant t. A MUMPS (MUltifrontal Massively Parallel sparse direct Solver) solver is used to obtain the solution in both studies. The resonance frequency values are normalized using Eq. (12):

$$f_n = \frac{f_r}{f_{ss}} \tag{12}$$

where f_{ss} represents the steady state resonance frequency of the beam. From now on, this state in considered to be equivalent to a completely dry state, namely, a state when the concentration ϕ has returned to its initial state before interacting with the liquid.

3.2. Parametric analysis

From the formulation presented in Section 2, it can be noticed that the solution of the liquid-transport-elasticity model can be described with only 3 parameters: (i) the normalized sink/source term (F), (ii) the relaxation constant (β) and (iii) the ratio between wet and dry Young modulus of paper (m). However, it is necessary to investigate the influence of each parameter in the dynamic response of the model. Therefore, a parametric analysis is performed using the numerical approach described in Section 3.1. The parameter values used in this analysis are presented in Table 1.

The values for β and m are selected according to an analysis of Eq. (6). From this analysis it can be observed that the increment β could lead to a quasi-instantaneous drying response. Therefore, values greater than $\beta = 16$ are avoided. The values for m is selected according with the reported values of the Young modulus of paper in saturated state [12,14]

3.3. Experimental validation

The validation of the parametric model is performed in this section by experiments described below. The experimental procedure can be summarized in the following steps:

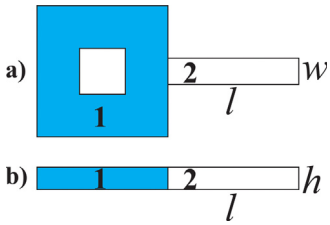

Fig. 2. Paper-based cantilever beam sample configuration (a) Top view, (b) Lateral view.

(1) Fabrication of the paper-based sample
(2) Measurement of the resonant frequency of the sample by experiments described in this section
(3) Develop a model of the sample beam response using an error minimization approach

3.3.1. Sample fabrication

In order to study the dynamic response of paper when saturated with liquid, a set of samples are fabricated from Whatman® 3MM chromatography paper ($h = 340$ μm). This kind of paper has been used in the development of paper-based systems such as in [4,6]. Furthermore, its liquid transport behavior has been already studied in [15]. The configuration of the samples is shown in Fig. 2. The samples consist of 2 domains, the fixed domain (1) and the flexing beam domain (2). The samples are fabricated with rectangular-cross section and a length $l = 10$ mm and a width of $b = 2$ mm. A hydrophobic region on the samples at the clamping part is created while the rest of the beam is left as a hydrophilic region. A Xerox® ColorQube 8570 printer is used to deposit a wax layer on top of the samples (domain 1, Fig. 2). Then, the samples are baked on an electric heated oven at a temperature of 115 °C for 8 min. This process is performed to melt the wax and make it penetrate throughout the thickness h forming the hydrophobic region. This procedure to form hydrophobic regions with melted wax has already been used in the development of microfluidic devices such as in [18].

3.3.2. Measurement of the paper-based cantilever beam dynamic response

The paper samples are stored in a controlled environment chamber set to 60% of relative humidity and 25 °C for 24 h to ensure a uniform moisture content in the samples. All the experiments are carried out in the system described in [19]. A set of three distilled water–ethanol solutions with ethanol at 0%, 25% and 50% (v/v) are prepared to validate the model. The saturation volume V_s for the paper sample is calculated to determine the required volume of solution for the experiments with Eq. (13) [20]:

$$P_t\,(\%) = \frac{(m_{sat} - m_{dry})/\rho_{sol}}{V_a} \tag{13}$$

where m_{sat} is the mass of the saturated paper sample, m_{dry} is the mass of the dry paper sample, ρ_{sol} is the solution density, V_a is the apparent volume of the paper sample and P_t is the porosity of the sample. The numerator of Eq. (13) represents the liquid volume necessary to saturate the sample (V_{sol}); hence, it can be rewritten as follows:

$$V_{sol} = V_a P_t \tag{14}$$

A porosity value of 68.48% for the chromatography paper is used [19]. Therefore, a value of $V_{sol} = 4.7$μL is used to saturate the domain 2 of the samples. This volume is used in all the experiments, assuming this volume saturates the domain 2 of the samples. From a series of preliminary experiments, it is determined that a time period of 4800 s is necessary to study the complete drying phenomena from saturated to dry.

The measurement procedure to obtain the resonance frequency of the sample is summarized in the following steps:

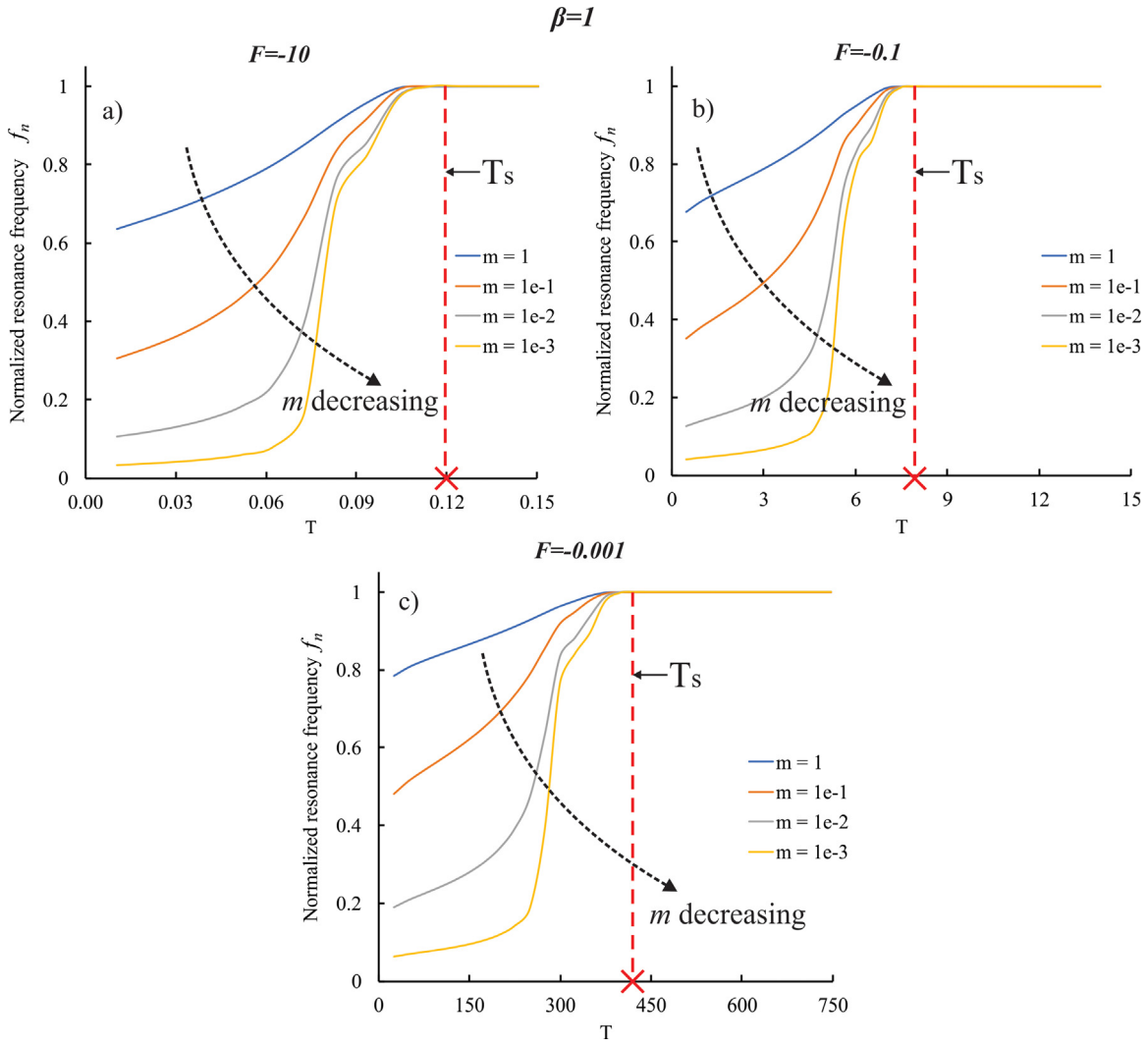

Fig. 3. Normalized resonance frequency of the beam for $\beta = 1$ (a) $F = -10$ 1/s; (b) $F = -0.1$ 1/s; (c) $F = -0.001$ 1/s.

(1) A paper sample is placed and mounted on the resonance frequency measurement system described in [19].
(2) A micropipette is used to place a volume V_{sol} of solution in one spot located at the top center of the beam.
(3) A pure mechanical harmonic excitation is used to obtain the resonance frequency of the sample on the first flexural mode. The resonance frequency of the sample is monitored for 4800 s.

3.3.3. Model approximation

The experimental resonance frequency is also normalized to the dry resonance frequency obtained in the numerical results (f_{ss}) using Eq. (12). A fitting curve procedure is then applied to the 3 experimental results to obtain an approximated model with the parameters F, β and m. An RMS error minimization approach is then used to tune the model parameters that better describes the experimental results.

4. Results and discussion

In this section, the results for the parametric analysis are presented and the influence of each model parameter over the model response is discussed. The experimental validation results are presented, and the accuracy of the model is discussed by analyzing the error between the numerical solution and the experimental results for each liquid solution.

4.1. Parametric analysis

Figs. 3 and 4 represent the dynamic response of the cantilever beam. For this analysis, the individual influence of 2 parameters related with the nonlinear relaxation (β and m) and one related to the liquid transport (F) are considered. In Fig. 3, the parametric analysis corresponding to the combinations of parameters for $\beta = 1$ are represented in three plots, each one corresponding to different values of F. Each plot shows the time variation of the normalized resonance frequency f_n for 4 selected values of m. It can be noticed from these plots that when the value of m is decreased, the initial value of f_n is also decreased; thus, modifying the shape of the curve. However, it can be noted in Fig. 3a that the steady state time T_s is not affected when the value of m is changed. This statement also applies when $F = -0.1$ and $F = -0.001$ that corresponds to Figs. 3b and 3c respectively. It can be also noticed that the families of curves are similar for the three values of F.

In Fig. 4, the parametric analysis for $\beta = 8$ are shown. From these plots, some interesting points should be noticed. The family of curves are similar for the three values of F and the time T_s is also increased with decreasing values of F. However, it should be observed that the increment in β produces a greater decay in the initial frequency of f_n. This phenomenon can be observed in the 3 plots of Fig. 3 when compared with the family of curves obtained with $\beta = 1$. An additional comparison can be done by observing the behavior of T_s in Figs. 3 and 4. For instance, it can be observed that T_s is the same in Figs. 3a and

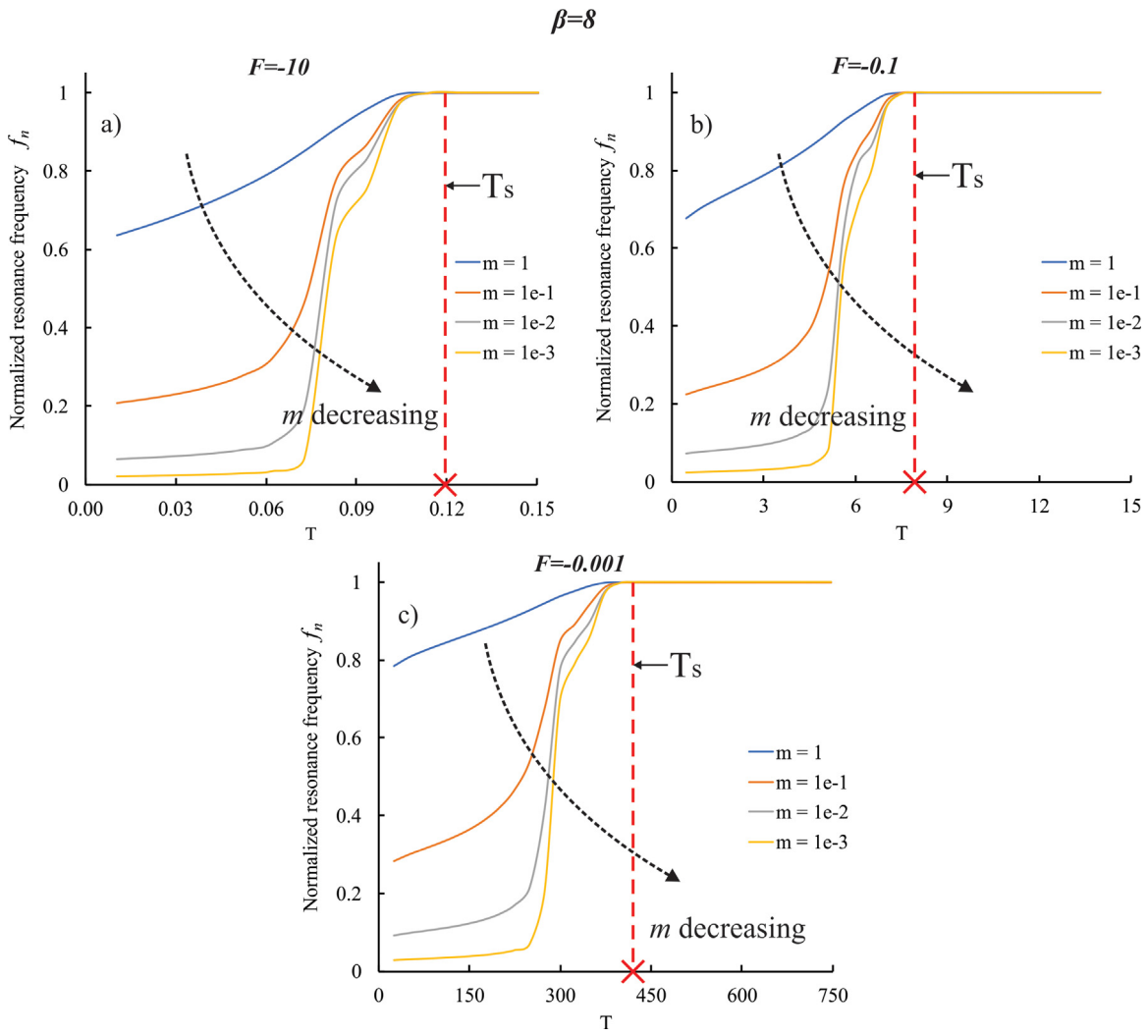

Fig. 4. Normalized resonance frequency of the beam for $\beta = 8$ with different values of F (a) $F = -10$ 1/s; (b) $F = -0.1$ 1/s; (c) $F = -0.001$ 1/s.

4a where $F = -10$. A similar statement can be done about the pair of plots with $F = -0.1$ and $F = -0.001$. Therefore, it can be concluded that F changes the time-scale of the dynamic response.

From a physical point of view, the plots in Figs. 3 and 4 can be used to represent the drying process of a paper-based cantilever beam, from the saturation state to the dry state. The time T_s can be used in this context to characterize the drying time. It is interesting to point out that this drying time is incremented when the magnitude of F is also incremented. This magnitude is related with the liquid flow to the external surrounding media; therefore, greater magnitudes of F imply a greater outflow of liquid from the sample.

The decrease in the values of the ratio m can be physically interpreted as a liquid having a greater softening effect on paper. This effect is evidenced by the initial value of the normalized resonance frequency f_n, as this value is proportional to the stiffness of the sample. Special attention should be paid to the cases where $m = 1$ from a physical point of view, representing a situation where a liquid has no effect on the Young modulus value. The case of $m = 1 \times 10^{-3}$ represents a situation where a liquid causes the reduction of the paper Young modulus in three orders of magnitude when saturated. In comparison, some authors have experimentally determined the value of m for different types of paper. For instance, Douezan et al. obtained a value of $m = 2.4 \times 10^{-1}$ for tracing paper [12]; while Lee et al. determined a value of $m = 2.9 \times 10^{-2}$ for Whatman filter paper [13]. It can be observed that these cases are covered with the range of values selected for this study. The effect of the relaxation constant β can be seen from Fig. 4. It should be noticed that this parameter affects the dynamics of the transition from the saturated state to the dry state.

Table 2
Values of T_s for the magnitude of F.

$\lvert F \rvert$	T_s
0.001	423.52
0.01	56.05
0.1	7.94
1	1.05
10	0.12
100	0.013

The previous analysis is extended to 6 different values of F in order to determine the relationship between the sink/source term F and the time T_s. The values of $|F|$ and their corresponding values of T_s are presented in Table 2. In this study, T_s is obtained as the first instant in which the resonance frequency has reached a steady value ($f_n = 1$) in the numerical solution.

From Table 2, the value of T_s is observed to decrease with the magnitude of the normalized sink/source term F. This validates the fact that a greater liquid outflow accelerates the drying process. From a curve fitting analysis of this data, it is evident that the drying time T_s has a nonlinear relationship with the sink/source term. From the physical point of view, it can be stated that the drying time has an exponential dependence on the outflow of liquid from the sample. A

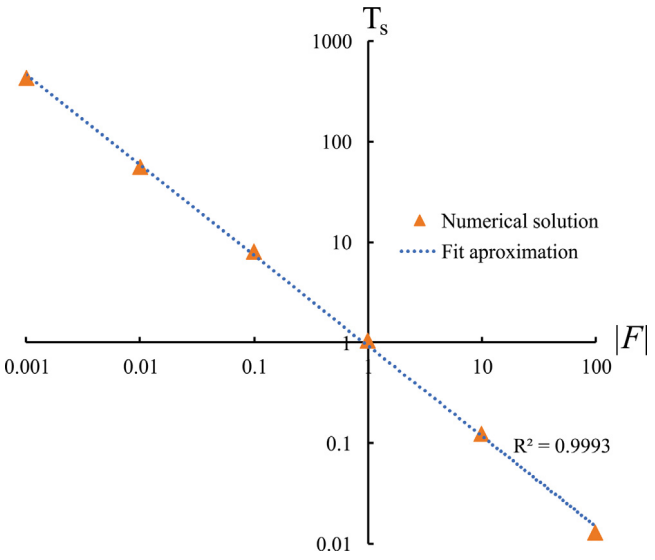

Fig. 5. Log–log scale plot for the function that represents the behavior of T_s with the magnitude of F.

10-base logarithmic scale x-y plot is presented in Fig. 5, showing a high linear behavior when analyzed in this scale ($R^2 = 0.9993$). From this analysis, it can be observed that higher values of F should be used to model a faster drying process in paper.

4.2. Experimental validation

In Fig. 6, the comparison between the experimental and numerical results for the 3 binary solutions is presented. The continuous line represents the numerical solution of the problem, and the dotted line represents the experimental measurements. The drying time T_s is determined for each solution in order the drying process of each solution. For the 3 solutions, a drying time T_s of 1.7×10^5, 1.21×10^5 and 1.07×10^5 are obtained for the 0%, 25% and 50% ethanol solutions respectively. These results indicate that greater concentration of ethanol produces a faster drying process in the paper samples; agreeing with the fact that ethanol has a higher volatility than water. It must be remarked that the volatility depends on the strength of the liquid intermolecular bonds. The water molecules have stronger intermolecular bonds when compared to ethanol. Therefore, it is easier for ethanol to break the interface between liquid and gas when kinetic energy is added to the liquid. It can be concluded that solutions with greater ethanol content produce a faster drying process.

The resulting parameters for each binary solution are presented in Table 3. From the analysis of this Table, it can be observed that the values of β do not seem to be correlated with the ethanol content. It is interesting to notice that the magnitude of F increase with the content of ethanol; indicating that the output rate of liquid from paper to the surrounding media is faster when the ethanol content in the solution is increased. From the values m, it is important to notice that this parameter increases when the ethanol content is increased in the solution. As m is related to the relaxation of the Young modulus, it can be concluded that water causes a greater relaxation effect on paper than ethanol.

The accuracy of the approximated models is evaluated after running error analysis for each binary solution. The numerical and experimental results are compared obtaining an error function with Eq. (14)

$$e_a(t) = f_n(t) - r_{ex}(t) \tag{15}$$

where e_a is the absolute error at an instant t and r_{ex} is the normalized experimental resonance frequency.

Table 3
Fitted parameters for water–ethanol solutions.

Solution	Parameters		
	β	m	F
Ethanol 0%	1.1	1.3e−2	−9.0e−7
Ethanol 25%	1.0	1.7e−2	−1.3e−6
Ethanol 50%	1.0	3.0e−1	−1.2e−5

The error functions are illustrated in Fig. 7a to c. It can be observed from this Figure that the error does not have a magnitude greater than 6% in each case. The maximum magnitude of error is computed for each binary solution, obtaining values of 4.0%, 3.6% and 5.2% respectively. The RMS error is computed with Eq. (15)

$$e_{RMS} = \sqrt{\frac{\sum_{i=1}^{n}(f_n - r_{ex})^2}{n_d}} \tag{16}$$

where n_d represents the number of samples. The RMS error values obtained are 1.8%, 1.5% and 2.1%, further validating the accuracy of the study.

It must be noted that, for this parametric study, the hygroexpansion strain of paper is discarded in the analysis. According to the observations made in [12,13], the maximum hygroexpansive strain in paper ranges from 3.5% to 10%. Therefore, a theoretical analysis is addressed in order to determine the effect on the resonance frequency due to thickness variation alone; obtaining an increment of 15%. However, it must be noted that the sample thickness is not constant through the drying process; as it depends on the liquid concentration. The accuracy of the model could be improved in future analysis if these factors are considered.

5. Conclusions

In this paper, a parametric study that describes the nonlinear dynamic response of paper when interacting with water-based liquids is presented. A three-dimensional numerical model is used to describe the physics of paper with three parameters, coupling the nonlinear Richard's model of liquid transport with an elasticity model. The elasticity model is formulated considering the nonlinear effects of paper relaxation and liquid transport on the behavior of the Young modulus. The influence of these parameters in the dynamic response of paper is determined: the normalized sink/source term F is related to the drying time of the paper sample; m determines the initial resonance frequency and β determines the dynamics of the transition from saturated to dry. The drying process of paper is accurately modeled; this can be proved by the accurate response obtained for three different binary solutions. An error analysis is performed, obtaining a relatively small error given the complexity and nonlinearity of the liquid transport physics. This work can provide some means of producing low cost devices such as liquid characterization sensors and wearable devices.

Declaration of competing interest

The authors declare that they have no known competing financial interests or personal relationships that could have appeared to influence the work reported in this paper.

CRediT authorship contribution statement

Isaias Cueva-Perez: Data curation, Formal analysis, Investigation, Software. **Angel Perez-Cruz:** Conceptualization, Data curation, Formal analysis, Funding acquisition, Methodology, Project administration, Resources, Validation, Visualization. **Ion Stiharu:** Conceptualization. **Aurelio Dominguez-Gonzalez:** Funding acquisition, Resources. **Miguel Trejo-Hernandez:** Visualization. **Roque Alfredo Osornio-Rios:** Funding acquisition, Investigation, Methodology, Project administration, Resources, Supervision, Visualization.

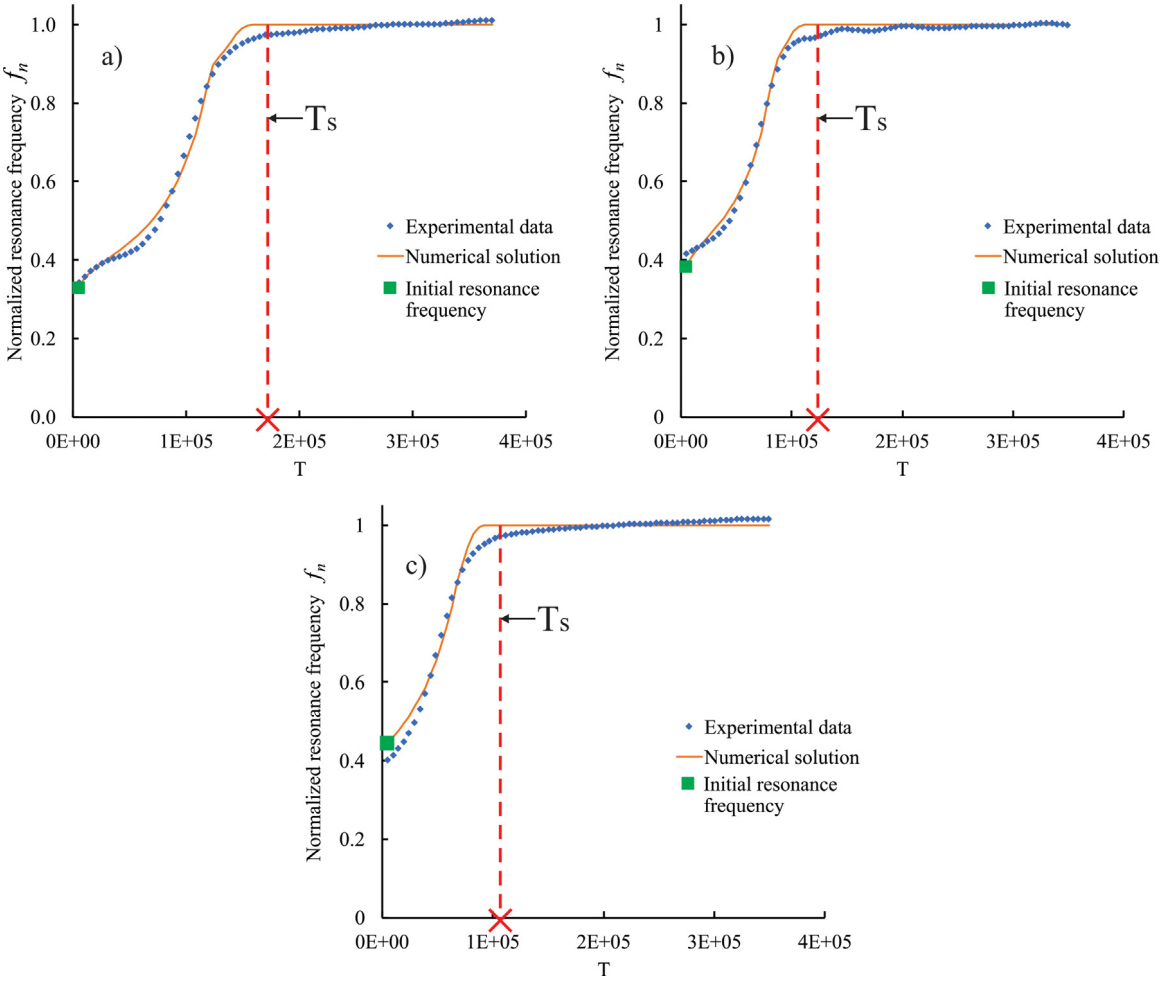

Fig. 6. Experimental results with numerical approximation. (a) Ethanol 0%; (b) Ethanol 25% and (c) Ethanol 50%.

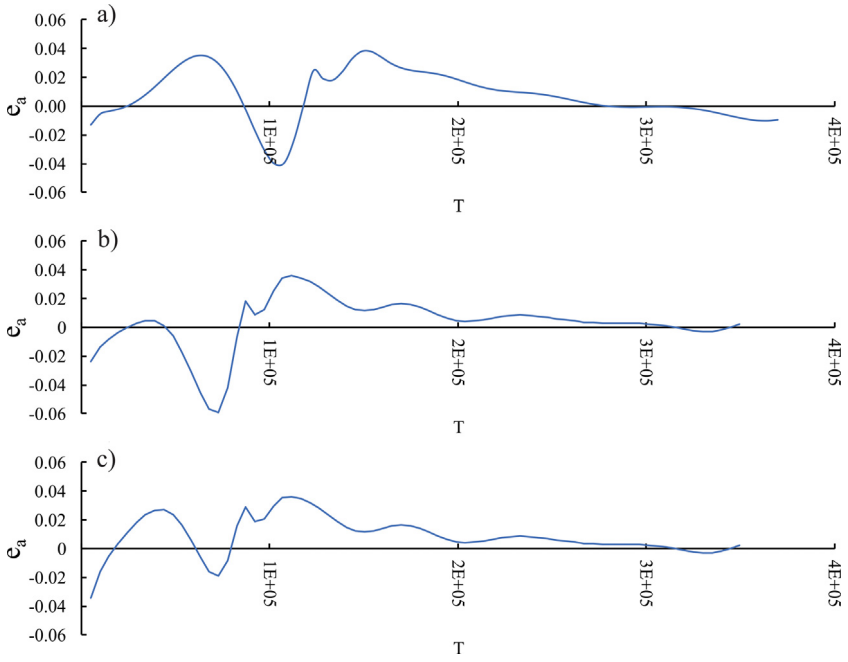

Fig. 7. Absolute error for (a) Ethanol 0%; (b) Ethanol 25% and (c) Ethanol 50%.

Acknowledgments

This work was supported by the CONACyT (Consejo Nacional de Ciencia y Tecnología), Mexico scholarship number 591667/304869 and the project FOFIUAQ-2018 (grant number FIN201903).

References

[1] J. Kim, J.-Y. Kim, S. Choe, Electroactive papers: possibility as actuators, in: Smart Struct. Mater. 2000 Electroact. Polym. Actuators Devices, Vol. 3987, 2003, p. 203, http://dx.doi.org/10.1117/12.387779.

[2] Z. Ding, P. Wei, G. Chitnis, B. Ziaie, Ferrofluid-impregnated paper actuators, J. Microelectromech. Syst. 20 (2011) 59–64, http://dx.doi.org/10.1109/JMEMS.2010.2100026.

[3] A. Fraiwan, H. Lee, S. Choi, A paper-based cantilever array sensor: Monitoring volatile organic compounds with naked eye, Talanta 158 (2016) 57–62, http://dx.doi.org/10.1016/j.talanta.2016.05.048.

[4] X. Liu, M. Mwangi, X. Li, M. O'Brien, G.M. Whitesides, Paper-based piezoresistive MEMS sensors, Lab Chip 11 (2011) 2189–2196, http://dx.doi.org/10.1039/c1lc20161a.

[5] T.L. Ren, H. Tian, D. Xie, Y. Yang, Flexible Graphite-on-Paper piezoresistive sensors, Sensors 12 (2012) 6685–6694, http://dx.doi.org/10.3390/s120506685 (in Switzerland).

[6] Y.H. Wang, P. Song, X. Li, C. Ru, G. Ferrari, P. Balasubramanian, M. Amabili, Y. Sun, X. Liu, A paper-based piezoelectric accelerometer, Micromachines 9 (2018) http://dx.doi.org/10.3390/mi9010019.

[7] A.L. Erkkilä, T. Leppänen, J. Hämäläinen, T. Tuovinen, Hygro-elasto-plastic model for planar orthotropic material, Int. J. Solids Struct. 62 (2015) 66–80, http://dx.doi.org/10.1016/j.ijsolstr.2015.02.001.

[8] H. Gao, F. Wang, Z. Shao, Study on the rheological model of Xuan paper, Wood Sci. Technol. 50 (2016) 427–440, http://dx.doi.org/10.1007/s00226-015-0781-1.

[9] Y. Li, S.E. Stapleton, S. Reese, J.W. Simon, Anisotropic elastic–plastic deformation of paper: Out-of-plane model, Int. J. Solids Struct. 130–131 (2018) 172–182, http://dx.doi.org/10.1016/j.ijsolstr.2017.10.003.

[10] A.K.I. Hall, T.C. O'Connor, M.K. McGath, P. McGuiggan, The bending mechanics of aged paper, J. Appl. Mech. 85 (2018) 071005, http://dx.doi.org/10.1115/1.4039881.

[11] C. Carrell, A. Kava, M. Nguyen, R. Menger, Z. Munshi, Z. Call, M. Nussbaum, C. Henry, Beyond the lateral flow assay: A review of paper-based microfluidics, Microelectron. Eng. 206 (2019) 45–54, http://dx.doi.org/10.1016/j.mee.2018.12.002.

[12] S. Douezan, M. Wyart, F. Brochard-Wyart, D. Cuvelier, Curling instability induced by swelling, Soft Matter. 7 (2011) 1506–1511, http://dx.doi.org/10.1039/c0sm00189a.

[13] E. Reyssat, L. Mahadevan, How wet paper curls, Europhys. Lett. 93 (2011) http://dx.doi.org/10.1209/0295-5075/93/54001.

[14] M. Lee, S. Kim, H.Y. Kim, L. Mahadevan, Bending and buckling of wet paper, Phys. Fluids 28 (2016) http://dx.doi.org/10.1063/1.4944659.

[15] A. Perez-Cruz, I. Stiharu, A. Dominguez-Gonzalez, Two-dimensional model of imbibition into paper-based networks using Richards' equation, Microfluid. Nanofluid. 21 (2017) 1–12, http://dx.doi.org/10.1007/s10404-017-1937-0.

[16] A. Perez-Cruz, I. Stiharu, A. Dominguez-Gonzalez, Nonlinear imbibition influence on the hygro-mechanical bending response of paper due to its interaction with water, Int. J. Non-Linear Mech. 97 (2017) 89–95, http://dx.doi.org/10.1016/j.ijnonlinmec.2017.09.002.

[17] S. Schmid, S. Kühne, C. Hierold, Influence of air humidity on polymeric microresonators, J. Micromech. Microeng. 19 (2009) http://dx.doi.org/10.1088/0960-1317/19/6/065018.

[18] T. Tian, X. Wei, S. Jia, R. Zhang, J. Li, Z. Zhu, H. Zhang, Y. Ma, Z. Lin, C.J. Yang, Integration of target responsive hydrogel with cascaded enzymatic reactions and microfluidic paper-based analytic devices (μPADs) for point-of-care testing (POCT), Biosens. Bioelectron. (2016) http://dx.doi.org/10.1016/j.bios.2015.09.049.

[19] I. Cueva-Perez, R.A. Osornio-Rios, I. Stiharu, A. Perez-Cruz, Extraction of nonlinear elastic parameters of paper from the amplitude-dependent frequency response of cantilever beams, Int. J. Non-Linear Mech. 111 (2019) 42–48, http://dx.doi.org/10.1016/j.ijnonlinmec.2019.01.017.

[20] J.E. Unosson, C. Persson, H. Engqvist, An evaluation of methods to determine the porosity of calcium phosphate cements, J. Biomed. Mater. Res. B 103 (2015) 62–71, http://dx.doi.org/10.1002/jbm.b.33173.